Dalton Transactions

An international journal of inorganic chemistry

Accepted Manuscript

This article can be cited before page numbers have been issued, to do this please use: L. You, S. Yao, B. Zhao, G. Xiong, I. Dragutan, V. Dragutan, X. liu, F. Ding and Y. Sun, *Dalton Trans.*, 2020, DOI: 10.1039/D0DT00770F.

ROYAL SOCIETY OF CHEMISTRY

rsc.li/dalton

View Article Online
DOI: 10.1039/D0DT00770F

ARTICLE

Striking dual functionality of the novel Pd@Eu-MOF nanocatalyst in C(sp^2)-C(sp^2) bond-forming and CO_2 fixation reactions

Received 00th January 20xx,
Accepted 00th January 20xx

DOI: 10.1039/x0xx00000x

Li-Xin You,[a] Shan-Xin Yao,[a] Bai-Bei Zhao,[a] Gang Xiong,[a] Ileana Dragutan,[b] Valerian Dragutan,*[b] Xue-Gui Liu,[c] Fu Ding[a] and Ya-Guang Sun*[a]

Pd nanoparticles were immobilized on a highly porous, hydrothermally stable Eu-MOF via solution impregnation and H_2 reduction to yield a novel Pd@Eu-MOF nanocatalyst. This composite was characterized by scanning electron microscopy (SEM), transmission electron microscopy (TEM), energy dispersive spectroscopy (EDS), inductive coupled plasma optical emission spectroscopy (ICP), powder X-ray diffraction (PXRD) and X-ray photoelectron spectroscopy (XPS). Unprecedentedly, the Pd@Eu-MOF nanocatalyst could be applied with excellent results in two strikingly different, mechanistically distinct, reactions i.e., Suzuki-Miyaura cross-coupling and cycloaddition of CO_2 to a range epoxides. Under best reaction conditions, 98-99% yields have been attained in both catalytic processes. Moreover, in either case the heterogeneous catalyst was easily recovered and efficiently reused for more than four cycles indicating its high stability and reproducible activity. PXRD, TEM and XPS measurements on the recycled catalyst confirmed that it has maintained its original structure and morphology; no Pd NPs agglomeration was evidenced.

Introduction

Metal organic frameworks (MOFs), also known as porous coordination polymers, are well-ordered crystalline materials assembled from metal nodes and organic linkers.[1] MOFs have attracted a substantial interest in recent years due not only to their easy synthesis and versatility in structure, but also to their application profile in different fields such as energy storage,[2] gas adsorption and separation,[3] luminescence,[4] magnetism[5] and catalysis.[6a-c] and even integration on protective layers against dangerous agents.[6d]

MOFs have been directly used in the realm of heterogeneous catalysis owing to their assets i.e. large specific surface area, controllable pore size, easily accessible catalytic sites, high stability, and recoverability.[7] In addition, MOFs can be used as novel supports to incorporate metal nanoparticles (NPs).[8] The NPs hosted inside MOF can act as active sites, while the pores of the MOF stabilize the NPs size and impede their leaching and growth during operation of the catalytic systems. To be used as hosts, MOFs should be sufficiently robust to withstand the reaction conditions. The migration of NPs is greatly limited in MOFs, so the stability and activity of the catalyst are preserved. Recently, our group[9a-d] and others[9e-h] have successfully applied the Pd-based MOFs in Suzuki-Miyaura cross-coupling reaction of aryl halides with arylboronic acids, as one of the most widely employed methods for the construction of C(sp^2)-C(sp^2) bonds because of its broad substrate scope, high level of functional group tolerance and high turnover rates.[9i,j] Development of recoverable and recyclable heterogeneous catalysts is still a serious challenge, when compared with the homogeneous palladium catalysts. In addition, the chemical fixation and conversion of carbon dioxide (CO_2) to structurally diverse compounds has received much attention in last decades since CO_2 is abundant, renewable and inexpensive C1 building block from the green chemistry and atom economy viewpoints.[10] Cyclic carbonates resulted from the cycloaddition of CO_2 and epoxides are considered as one of the most significant types of targeted substances due to the relatively high yields and broad applications in fine chemicals, pharmaceuticals and medication syntheses.[11]

In this paper, Pd NPs have been loaded on the matrix of a highly porous and hydrothermally stable Eu-MOF, namely $\{[Eu_2(L)_3\bullet(H_2O)_2\bullet(DMF)_2]\bullet16H_2O\}_n$,[12a] based on the 1,4-bis(5-carboxy-1*H*-benzimidazole-2-yl)benzene ligand (H_2L), A solution impregnation method followed by H_2 reduction was chosen to obtain a new Pd@Eu-MOF catalyst with Pd NPs sizes ranging between 2-5 nm. Moreover, valorisation of this new catalyst in recyclable Suzuki-Miyaura cross-coupling reactions between aryl halides and phenylboronic acids, as well as in the chemical fixation of CO_2 to epoxides yielding cyclic carbonates were studied.

[a] Key Laboratory of Inorganic Molecule-Based Chemistry of Liaoning Province, Shenyang University of Chemical Technology, Shenyang 110142, China. E-mail: sunyaguang@syuct.edu.cn.
[b] Institute of Organic Chemistry, Romanian Academy, Bucharest, P. O. Box 35-108, 060023, Romania. E-mail: vdragutan@yahoo.com.
[c] Institute of Functional Molecules, Shenyang University of Chemical Technology, Shenyang 110142, China

† Electronic Supplementary Information (ESI) available: Representation of the PXRD diagrams, EDS spectrum, ^{1}H NMR data and GC-yield Standard Curves for the products. See DOI:10.1039/x0xx00000x

Experimental

Synthesis of the catalyst

All starting materials and solvents were obtained from commercial suppliers and used without further purification. The overall synthesis route of Pd@ Eu-MOF is shown in Scheme 1.

Synthesis of Eu-MOF Eu-MOF was obtained according to literature by reacting H_2L (0.0398 g, 1.0 mmol) with europium nitrate (0.0446 g, 1.0 mmol) in a mixture of DMF (5.0 mL) and H_2O (5.0 mL) at 120 °C for 72 h.[12a] Yellow crystals were collected by filtration, washed with water and dried in the air.

Synthesis of Pd@Eu-MOF The activated Eu-MOF (0.393 g, 0.2 mmol) and $PdCl_2$ (0.035 g, 0.2 mmol), were suspended in methanol (100.0 mL), and stirred for 24 h. The mixture was filtered and washed 3 times with fresh methanol (20.0 mL) and deionized water (20.0 mL). The solid (Pd/Eu-MOF) was dried under vacuum for 24 h at 45°C, and reduced at 60 °C, for 12h, in a flow of H_2/N_2 (10/40) mL min^{-1}. The product was washed with methanol and dried for 24 h at 45 °C to obtain the Pd@Eu-MOF catalyst.

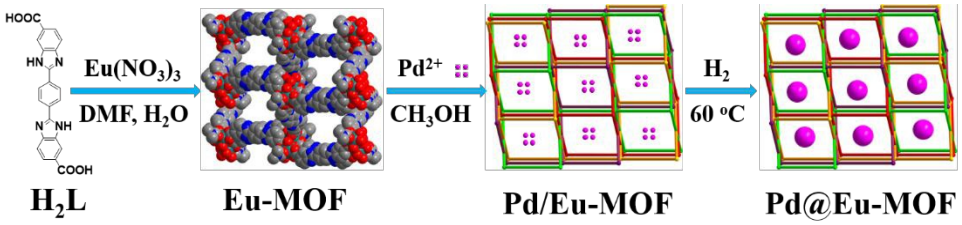

Scheme 1 Synthesis route of Pd@Eu-MOF.

Structural characterization of Pd@Eu-MOF. GC analysis

Powder X-ray diffraction (PXRD) of the sample was acquired on a BRUKER D8 ADVANCE X-ray diffractometer. N_2 gas sorption experiments were carried out on a V-Sorb 2800 TP volumetric gas sorption instrument. X-ray photoelectron spectroscopy (XPS) data were obtained on Axis Ultra DLD devices. Inductive coupled plasma optical emission spectroscopy (ICP) was accomplished on Thermo IRIS Advantage. Scanning electronmicroscope (SEM) images were taken with a German ZEISS-SUPRA55 high resolution field emission scanning electron microscope. Energy-dispersive X-ray spectroscopy (EDS) was achieved on a German ZEISS-SUPRA55 high resolution field emission scanning electron microscope with an Oxford-AztecX-Max80 X-ray energy spectrometer. Transmission electron microscopy (TEM) was measured by a TECNAI F30 imaging spectrometer; ^{1}H NMR spectra were recorded on a Bruker BioSpin GmbH AVANCE III 500 MHz spectrometer. Gas chromatography (GC) analyses were performed on an Agilent Technologies 7890A gas chromatograph.

Catalytic activity tests

Suzuki-Miyaura coupling reaction A typical experimental procedure for the Suzuki-Miyaura coupling reactions is as follows. A mixture of aryl halide (1.0 mmol), boronic acid(1.2 mmol), base (2.0 mmol, the indicated species), solvent (6.0 mL, as designated) and catalyst (the given amount) were placed in a Schlenk tube and stirred in air, at the appropriate temperature for the specified time (Tables 1, 2). After completion of the reaction the mixture was extracted with ethyl acetate. The product yield was determined by GC analysis using hexadecane as the internal standard.

Cycloaddition of CO_2 to epoxides yielding cyclic carbonates The epoxide (34.5 mmol) and catalyst (50.0 mg) were introduced into a stainless-steel autoclave. After sealing, the autoclave was purged 3 times with CO_2. Then, the pressure was adjusted to 2.0 MPa. After heating at 80 °C for 24 h, the reactor was cooled in an ice bath, and excess CO_2 was carefully vented off. The catalyst was separated by centrifugation, and the products were analyzed by GC. For recyclability tests of Pd@Eu-MOF, the catalyst was recovered by filtration and washed with hot methanol after each cycle.

Results and Discussion

Eu-MOF was readily synthesized by the solvothermal reaction according to the literature method.[12a] The PXRD patterns of the resulted solid matched well the calculated and literature[12] patterns (Fig. 1). They revealed the crystalline properties of the synthesized Eu-MOF to be properly utilized as a matrix for immobilization of Pd nanoparticles. The framework of Eu-MOF was chemically stable under aqueous sodium hydroxide and hydrochloric acid conditions (pH = 1-14) and in common organic solvents, as confirmed by the PXRD pattern collected for the respective samples (Fig. S1, 2). During the preparation of Pd@Eu-MOF there was no apparent loss of crystallinity and no identifiable peaks attributable to metal NPs, indicating that the Eu-MOF framework had maintained its structural integrity and that only very small NPs had been present in the Eu-MOF. Moreover, the stability of Pd@Eu-MOF was confirmed by PXRD after the reactions (Fig. S3).

The porosity of Pd@Eu-MOF was investigated by N_2 sorption measurement at 77 K. As indicated in Fig. 2, Eu-MOF, Pd/Eu-MOF and Pd@Eu-MOF show the typical type-I sorption isotherms, which reveal their microporous properties (Fig. S4). Pd@Eu-MOF displayed a slight decrease in the amount of adsorbed N_2, as compared to Eu-MOF and Pd/Eu-MOF. In addition, the Brunauer-Emmet-Teller (BET) surface area reduced from 1361 to 706 m^2 g^{-1} after Pd nanoparticles had been loaded (Table S1).

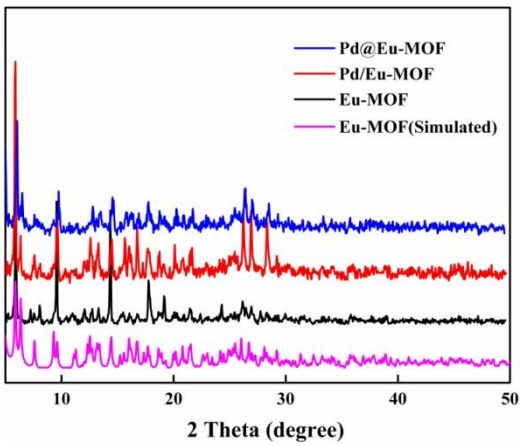

Fig. 1 PXRD patterns of different samples.

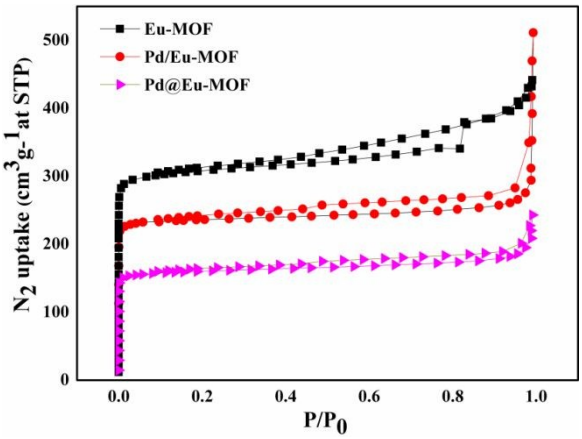

Fig. 2 N_2 adsorption/desorption isotherms of Eu-MOF, Pd/Eu-MOF and Pd@Eu-MOF.

The nanocomposite structure was investigated by EDS analysis, SEM and mapping images. The signals recorded in energy-dispersive X-ray spectroscopic measurements (EDS) identified the elements of Eu, Pd, Cl, C, N and O to be suitably displayed in the Pd@Eu-MOF nanocatalyst (Fig. 3).

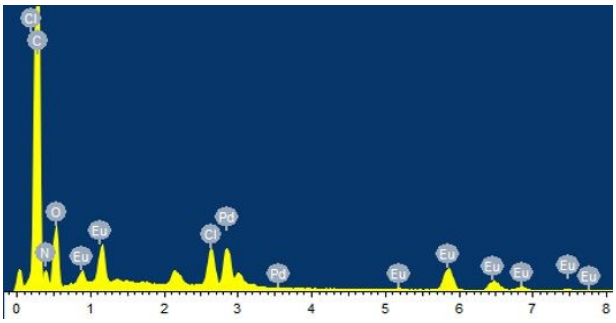

Fig. 3 EDS spectrum of Pd@Eu-MOF.

Additionally, SEM along with elemental mapping evidenced the adequate distribution of the constituent elements in the catalyst. Elemental maps indicated that Pd NPs were prepared in a regular and uniform manner, evidencing the presence of Eu, Pd, C, N and O in the respective samples (Fig. 4).

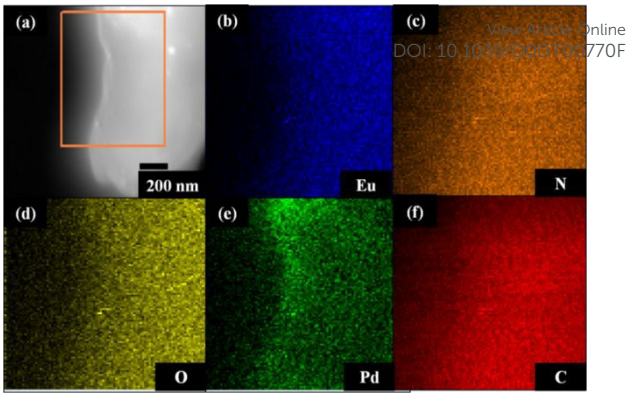

Fig. 4 SEM image (a) and elemental mappings of Pd@Eu-MOF shows the presence of Eu, N, O, Pd and C atoms (b-f).

As observed in the high-resolution TEM image, the morphology of Pd nanoparticles was spherical and completely dispersed and deposited inside the Eu-MOF, the particle size of Pd nanoparticles was found to be about 2-5 nm (Fig. 5a).

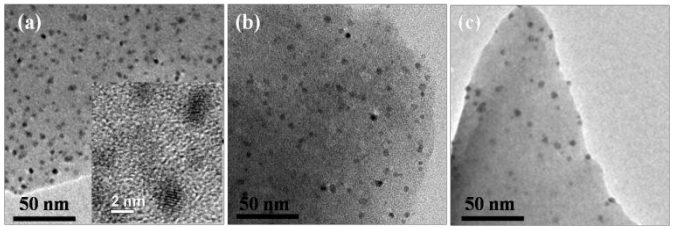

Fig. 5 TEM images of Pd@Eu-MOF before reaction (a), after Suzuki-Miyaura coupling reaction(b) and cycloaddition of CO_2 with epoxide (c).

In our work pore sizes between 0.7-2.7 nm have been evidenced for Pd@Eu-MOF (Fig. S4); this range is complying with the pore dimensions found for Eu-MOF(19x 12 A^2).[12a] Therefore, and as shown in Scheme 1 and confirmed by TEM experiments (Fig. 5), we infer that the majority of Pd NPs are located within the pores of Eu-MOF. These findings parallel those recently obtained by W.-Y. Sun[12b] for Pt nanoparticles inside a Zr-MOF.

Noteworthy, the TEM images of the recovered Pd@Eu-MOF after use in the Suzuki-Miyaura and CO_2 cycloaddition reaction (Fig. 5b and 5c, respectively), indicated that no agglomeration of the particles occurred and the morphology and size of the particles have not changed much in the recovered catalyst. These results proved that essentially no modification in the structure of Pd@Eu-MOF took place during the reaction.

The XPS spectra of Pd@Eu-MOF determined the oxidation states of Pd (Fig. 6). The peaks for binding energy of 334.97 and 340.22 eV demonstrated that Pd is present only in its reduced form, Pd^0. In addition, the valence of Pd species is restored to Pd^0 after the Suzuki-Miyaura (peaks at 335.09 and 340.31) and CO_2 cycloaddition (peaks at 335.28 and 340.64) reactions, respectively. ICP-AES was measured on IRIS Advantage; after calculation and analysis, the mass percentage of the Pd element in the catalyst Pd@Eu-MOF was 0.61 wt%.

View Article Online
DOI: 10.1039/D0DT00770F

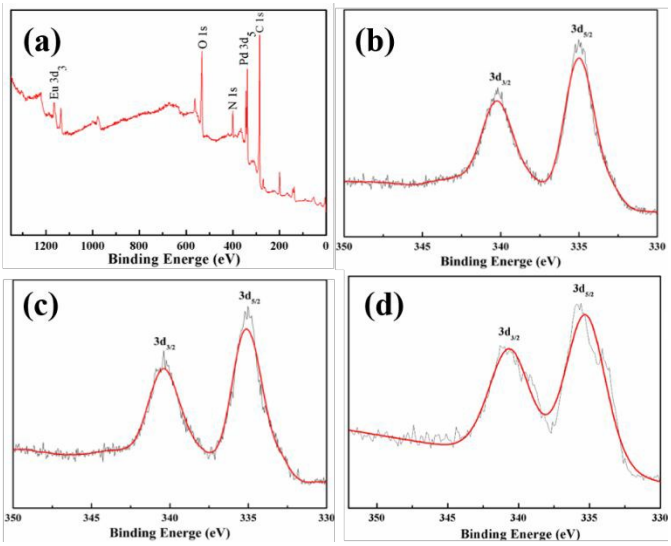

Fig. 6 XPS spectra of Pd@Eu-MOF before reaction(a); Pd 2p before reaction (b), after Suzuki-Miyaura coupling reaction(c) and cycloaddition of CO_2 with epoxide (d).

Table 1 Optimization of Suzuki-Miyaura cross-coupling of bromobenzene with phenylboronic acid in presence of Pd@Eu-MOF.

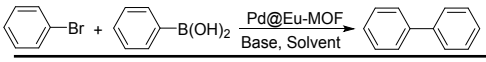

Entry	Solvent	Base	Time (h)	Temperature (°C)	Yield
1	DMF	K_2CO_3	6	80	36
2	Toluene	K_2CO_3	6	80	<5
3	H_2O	K_2CO_3	6	80	56
4	EtOH	K_2CO_3	6	80	99
5	EtOH	Cs_2CO_3	6	80	36
6	EtOH	NaOH	6	80	16
7	EtOH	Et_3N	6	80	56
8	EtOH	$NaOC_4H_9$-*t*	6	80	74
9	EtOH	K_2CO_3	6	70	89
10	EtOH	K_2CO_3	6	60	50
11	EtOH	K_2CO_3	6	50	32
12	EtOH	K_2CO_3	5	80	92
13	EtOH	K_2CO_3	4	80	86
14	EtOH	K_2CO_3	2	80	70

Reaction conditions: bromobenzene (1.0 mmol), phenylboronic acid (1.2 mmol), Pd@Eu-MOF (11.0 mg), base (2.0 mmol), solvent (6.0 mL).

Optimization of Suzuki-Miyaura cross-coupling reaction with Pd@Eu-MOF has been performed employing different bases and solvents (Table 1). It can be observed that the best combination leading to highest yield (>99%) was to use K_2CO_3 as the base and anhydrous ethanol as the solvent (Entry 4). When N,N-dimethylformamide (DMF), toluene and H_2O were used as a solvent instead of ethanol (Entry 1, 2, 3) or Cs_2CO_3, NaOH, sodium *t*-butoxide and triethylamine (Et_3N) as a base (Entry 5-8), the yield dropped significantly. Furthermore, reaction temperature and time affected notably the reaction yield (Entry 9-14). In conclusion, the optimum catalytic conditions for the Suzuki-Miyaura cross-coupling reaction of bromobenzene and phenylboronic acid are as follows: anhydrous ethanol as solvent, potassium carbonate as base, catalyst loading 11.0 mg, reaction time 6 h, temperature 80 °C.

On carrying out the cross-coupling of bromobenzene with phenylboronic acid, under the above optimum reaction conditions but using Pd@Eu-MOF, Pd/Eu-MOF and Eu-MOF as different promoters, quite interesting data were recorded (Table 2).

Table 2 Catalytic activity of Pd@Eu-MOF, Pd/Eu-MOF and Eu-MOF in Suzuki-Miyaura cross-coupling of bromobenzene with phenylboronic acid.

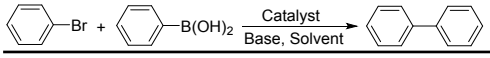

Entry	Halide (R_1/X)	Yield (%)
1	Pd@Eu-MOF	>99
2	Pd/Eu-MOF	81
3	Eu-MOF	<5

Reaction conditions: aryl halide (1.0 mmol), arylboronicacid (1.2 mmol), K_2CO_3 (2.0 mmol), EtOH (6.0 mL), catalyst (11.0 mg), temperature (80 °C), time (6 h).

The higher yield obtained with Pd@Eu-MOF (Table 2, Entry 1) could be rationalized if we take into account that the major part of Pd NPs is distributed inside the pores of Eu-MOF, the latter conferring, under such a protective confinement, superior activity and stability to the catalytic sites, preventing the Pd NPs aggregation and Pd leaching. It is noteworthy that the high yield in biaryls (>99%), attained in this work with Pd@Eu-MOF, is comparable to that reported recently by us in the Suzuki-Miyaura cross-coupling reaction using the nanostructured catalyst Fe_3O_4@La-MOF-Schiff base-Pd[8e] as well as in cross-couplings induced by Ln/Pd MOF catalysts [9a-d, 13b]

Table 3 Suzuki-Miyaura cross-coupling of various aryl halides with arylboronic acids.[a]

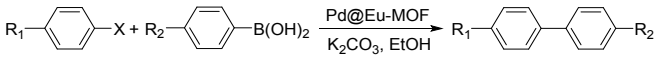

Entry	Halide (R_1/X)	Arylboronic acid (R_2)	Yield (%)
1	H/I	H	99
2	H/Br	H	99
3	CH_3/Br	H	90
4	$COCH_3$/Br	H	99
5	H/Br	$COCH_3$	87
6	H/Br	CH_3	99
7	$COCH_3$/Cl	H	14
8[b]	$COCH_3$/Cl	H	39

[a] Reaction conditions: aryl halide (1.0 mmol), arylboronic acid (1.2 mmol), K_2CO_3 (2.0 mmol), EtOH (6 mL), Pd@Eu-MOF (11.0 mg), temperature (80 °C), time (6 h). [b] Reaction conditions: reaction time: 12 h.

Significantly, the results obtained on the effect of substituents of arylhalides (Table 3) are in full agreement with the well-known data in this regard. The bromide and iodide derivatives react easier with phenylboronic acid to give higher yields (Entry 1-4). As expected, the yield of the chloride derivative was low (Entry 7), and only when the reaction time

was prolonged to 12 hours, the yield increased to 39% (Entry 8). These results are rationale taking into account the high activation energy needed for the chlorine derivative as compared to readily ionisable iodine and bromine counterparts, the last two involving a more electron-rich anionic [Pd(0)-X]-species in the rate-determining oxidative addition step of the palladium catalytic cycle[13a] (Scheme 2).

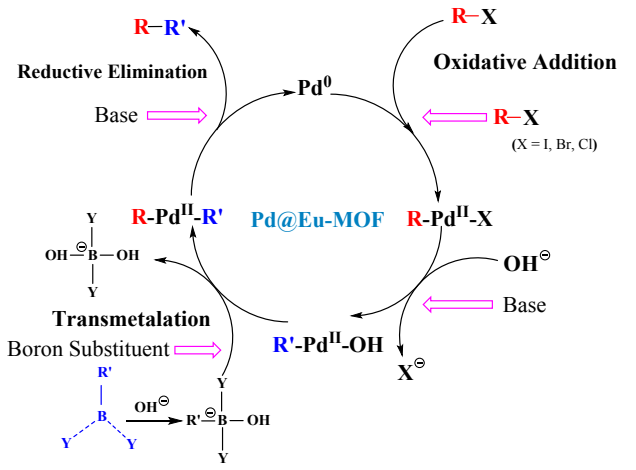

Scheme 2 Palladium catalytic cycle for C-C cross-coupling with Pd@Eu-MOF.

Tests with electron-donating (4-Me)-substituents (Entry 6) and electron-withdrawing substituents (4-COMe) (Entry 5) at the phenylboronic acid gave higher yields with 4-Me (> 99%) than with 4-COMe (87%), indicating that the catalyst is more prone to catalyze the reaction of phenylboronic acid with an electron donating substituent. This outcome is understandable if we consider the activating effect of the electron donating group on the ligand exchange rate within the boron complex during the transmetalation step of the pallacycle mechanism.[13b-f]

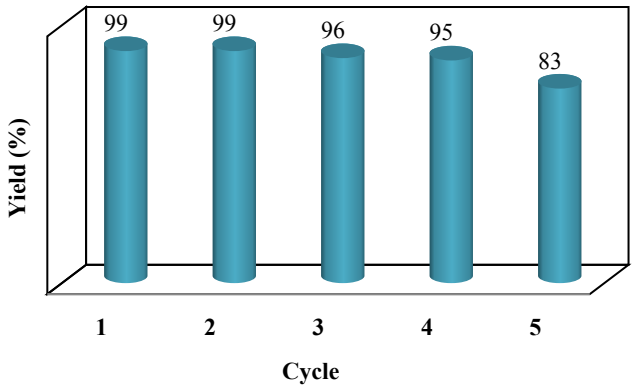

Fig. 7 Recycling of Pd@Eu-MOF in Suzuki-Miyaura cross-coupling reaction.

The recyclability of the heterogeneous catalyst is the most important advantage for industrial application. Catalyst recycling in Suzuki-Miyaura cross-coupling reaction of bromobenzene and phenylboronic acid was carried out under the optimum reaction conditions. After each reaction cycle, the catalyst was separated by centrifugation, washed with absolute ethanol, vacuumed at 50 °C and dried for the next run. Data on recycling of the Pd@Eu-MOF catalyst in Suzuki-Miyaura reaction are shown in Fig. 7. The catalytic results indicated that the Pd@Eu-MOF catalyst can be efficiently recycled showing almost no loss in activity for at least four successive runs.

A second catalytic ability of our Pd@Eu-MOF was also investigated, namely the technically and environmentally important CO_2 capture and conversion into value-added products[14a,b,c] such as the cyclic carbonates. Coupling with epoxides to yield cyclic carbonates (production: 40,000 tons/year) is in fact the major industrial catalytic utilization of CO_2.[15] Chemical fixation of CO_2 by cycloaddition to an epoxide proceeds through new C-O bond formation and is most frequently carried out heterogeneously with a MOF-supported metal catalyst. CO_2 capture by the epoxide is affected by its interaction with the MOF adsorbent. A prerequisite for successful catalysis is the occurrence on the MOF of densely dispersed Lewis acid and Lewis base sites (even as ILs, e.g. PolyILs@MIL-101),[16] as well as the presence of a co-catalyst, all of which playing essential roles in the different reaction stages.

Palladium, though since long applied in this reaction[17] is not often encountered among the host of metals used as catalysts. Moreover, Pd nanoparticles (supported on mesoporous TiO_2, Pd@$MTiO_2$) have only recently been communicated as catalysts in cyclic carbonate synthesis.[18]

In our case, the catalyst consists of Pd nanoparticles embedded in a microporous Eu-based MOF. To establish optimum reaction conditions with this new heterogeneous promoter, the solvent-free CO_2 cycloaddition to epichlorohydrin was selected as a model. As mandatory, a co-catalyst (*n*-Bu_4NBr) was also used. It was proved that Pd@Eu-MOF can convert CO_2 and epichlorohydrin to chloropropene carbonate in almost quantitative yields (98%), at 80 °C, 2.0 MPa CO_2 and 24 h reaction time, in the absence of any solvent (Table 4, entry 1). As indicated by previous research on cyclic carbonates synthesis using different catalysts, conversion is favoured by a higher operation temperature and pressure, the latter ensuring an increased solubility of CO_2;[19] in comparison to these data, a more advantageous molar ratio epoxide: catalyst (and epoxide:co-catalyst) could be established in this work.

Table 4 Synthesis of cyclic carbonates under different catalysis conditions.

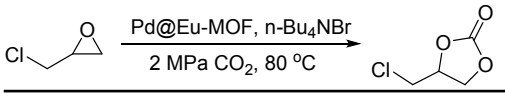

Entry	Catalyst	Cocatalyst (mg)	Yield (%)
1	Pd@Eu-MOF	100	98
2	Eu-MOF	100	38
3	Pd/Eu-MOF	100	42
4	-	100	46

Reaction conditions: epichlorohydrin (34.5 mmol), catalyst (50.0 mg), cocatalyst (*n*-Bu_4NBr, 100.0 mg), CO_2 pressure (2.0 MPa), temperature (80 °C), time (24 h). Yield was determined from GC analysis.

The reaction takes place with 46% conversion (Entry 4) even with just the co-catalyst (tetrabutylammonium bromide, TBAB) thus giving proof for the synergistic effect of the quaternary ammonium salt

during CO_2 cycloaddition (Scheme 3, path A). At the working temperature TBAB (m. p. 103 °C) is likely dissolved in the epoxide phase enhancing the CO_2 uptake. Control experiments using Eu-MOF and Pd/Eu-MOF, *i.e.* the MOF precursors of our catalyst, were also conducted leading to, not surprisingly, much poorer results (38% and 42%, respectively; entries 2 and 3). Europium is oxophilic yet, being relatively sparsely distributed and less exposed on the MOF surface, has lesser chances to attach the epoxide at the O atom; the same goes for Pd ions in the Pd/Eu-MOF.

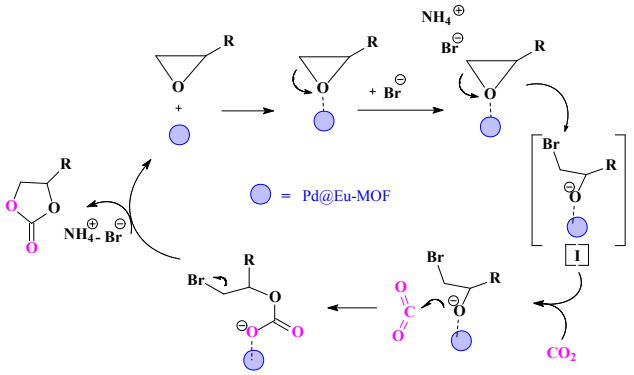

Scheme 3 Proposed mechanistic pathway for CO_2 insertion in the epoxide (Path A).

To explain our results with Pd@Eu-MOF in the coupling reaction of CO_2 and epichlorohydrin we propose a two-pathway mechanism (Scheme 3 – Path A and Scheme 4 – Path B) sharing the common intermediate [I]. According to the largely accepted pathway A,[20] first the oxygen atom of the epoxide binds to Lewis acid sites on the MOF activating the epoxy ring; then, Br^- (from *n*-Bu_4NBr) attacks the less-hindered C-atom of the now coordinated epoxide opening the epoxy ring and generating an O-anion [I]; the latter is subsequently attacked by CO_2 to yield a carbonate anion that ring-closes in the final step (Scheme 3).

The cooperative mechanism further implies participation of the intermediate [I] in a second reaction cycle (Path B) where it coordinates to Pd^0 nanoparticles (from Pd@Eu-MOF) yielding an anionic species able to bind two CO_2 molecules. On demand of ammonium cations, this species expels Br^- generating two cyclic carbonate molecules coordinated to palladium; ultimately, the reaction cycle B is closed by release of the cyclic carbonate in the reaction medium and restoration of the catalyst (Scheme 4).

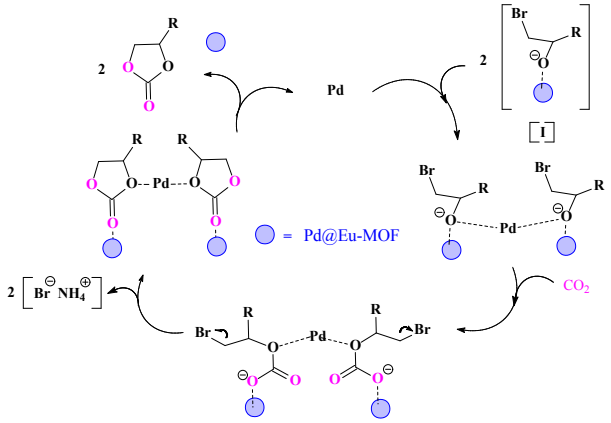

Scheme 4. Role of Pd nanoparticles in cyclic carbonates synthesis (Path B).

To conclude, the greatly enhanced catalytic performance of Pd@Eu-MOF, vs. Pd/Eu-MOF, results from the superior Lewis acid activity of the evenly distributed Pd nanoparticles (vs. Pd^{2+} ions), thus engendering an amplified coordination of the epoxide in the initial step of Path B. An unorthodox parallelism of the catalytic performance in the distinct reactions under study, Suzuki-Miyaura and cyclic carbonate synthesis (Table 2 and Table 4), shows the same trend for a decreasing activity in the range Pd@Eu-MOF > Pd/Eu-MOF > Eu-MOF, again revealing the positive role of Pd nanoparticle vs. Pd ions when either is incorporated in our catalytic MOF system.

The catalytic capacity and substrate selectivity of Pd@Eu-MOF were further explored using variously substituted epoxides to synthesize the corresponding cyclic carbonates, under the same reaction conditions. The size selectivity was evident when comparing the yields obtained from substrates with different substituents. The highest catalytic activity was observed when the substrate was phenyloxirane (yield of 90%; R = Ph, Entry 1, Table 5) or epichlorohydrin (yield 98%; R = $ClCH_2$, Entry 1, Table 4). Substituent effects, both steric and electronic, are therefore at play: bulkier substituents sterically hinder access of the epoxide to the catalytic centers whereas electron-withdrawing substituents facilitate nucleophilic attack of the base during ring opening of the epoxide. Therefore, CO_2 insertion is sensitive to the geometric and electronic environments of the epoxide, that govern the access of the substrate to the NP active sites inside the MOF, a conclusion shared by all previous reports on yield variation as a function of the epoxide R substituent.[21]

Table 5 Epoxide substrate in CO_2 fixation reactions catalyzed by Pd@Eu-MOF.

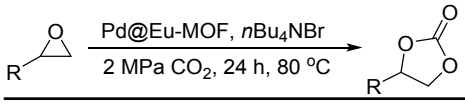

Entry	Substrate	Product	Yield (%)
1	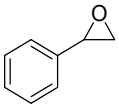	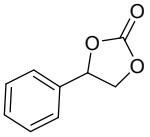	90
2		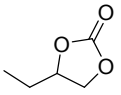	57
3			59
4	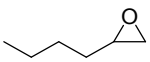	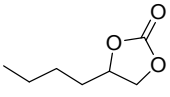	34

Reaction conditions: epoxide (34.5 mmol), Pd@Eu-MOF (50.0 mg), cocatalyst (*n*-Bu_4NBr, 100.0 mg), CO_2 pressure (2.0 MPa), temperature (80 °C), time (24 h). Yield was determined from GC analysis.

In this work insertion of CO_2 into epoxides was conducted as a solvent-free process which is an asset for a facile catalyst recovering

and recycling. After completion of the reaction the Pd@Eu-MOF catalyst could be efficiently separated from the mixture by centrifugation and reused in subsequent experiments showing no reduction of activity during the first 5 runs and just a slight decrease (to 93-94%) after the next two cycles (Fig. 8); therefore leaching of the active catalytic species was negligible.

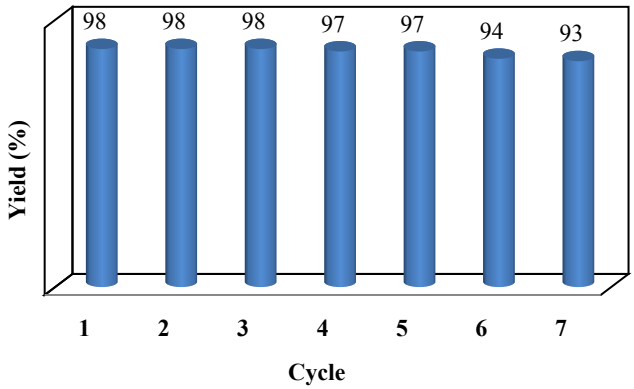

Fig. 8 Recycling of the Pd@Eu-MOF in the cycloaddition of CO_2 to epichlorohydrin.

The stability of Pd@Eu-MOF was confirmed from PXRD, TEM and XPS measurements following catalysis which showed that the catalyst has maintained its original crystalline structure and morphology after reactions (Fig. S3, 5, 6).

Conclusions

In summary, we have developed a robust and efficient heterogeneous catalyst Pd@Eu-MOF consisting of Pd nanoparticles immobilized in a europium metal-organic framework by using a solution impregnation and a subsequent gentle reduction approach. This method ensures control of the Bronsted to Lewis acid ratio in the material with effect on its catalytic propensity and selectivity. After reactions, Pd NPs do not aggregate in the Eu-MOF save guarding a high catalytic activity. The enhanced performance of Pd@Eu-MOF results from the superior Lewis acid propensity of the Pd nanoparticles, as compared to the Pd^{2+} ions in Pd/Eu-MOF.

We prove that the new Pd nanocatalyst exhibits an excellent dual catalytic behaviour: in Suzuki-Miyaura cross-coupling and cycloadditions of CO_2 to epoxides. In $C(sp^2)$-$C(sp^2)$ bond-forming reaction the Pd@Eu-MOF nanocatalyst led to high diaryl yields, under mild conditions. In CO_2 capture the nanocatalyst enabled synthesis of a diversity of cyclic carbonates. Chemical fixation of CO_2 is a promising method of utilizing this gas as a C-1 feedstock and one way to reduce global greenhouse emissions in the future, provided that more economically viable technologies for carbon capture are implemented.[22] Therefore, this study highlights a move towards sustainability and a way to deliver waste valorization. Work is underway for employing the Pd@Eu-MOF catalyst in other chemical transformations of practical utility.

Conflicts of interest

View Article Online
DOI: 10.1039/D0DT00770F

There are no conflicts of interest to declare.

Acknowledgements

This work was supported by the National Natural Science Foundation of China (21671139), the Distinguished Professor Project of Liaoning province (2013204), the National Key Research and Development Program of China (2018YFD0200102), the Scientific Research Project of Education Department of Liaoning Province (LDF2017001), the Program for Liaoning Innovative Research Team in University (LT2018012) and the Science and Technology Innovation Program for Middle-aged and Youth Talents of Shenyang (RC180086). ID and VD acknowledge support from the Institute of Organic Chemistry of the Romanian Academy.

Notes and references

1 (a) J. Y. R. Seow, W. S. Skinner, Z. U. Wang, H. L. Jiang, *Materialstoday*, 2019, **27**, 43; (b) Y.-Sh. Kang, Y. Lu, K. Chen, Y. Zhao, P. Wang, W.-Y. Sun, *Coord. Chem. Rev*., 2019, **378**, 262; (c) X. Chen, Y. Lyu, Z. Wang, X. Qiao, B. C. Gates, D. Yang, *ACS Catalysis*, 2020,**10**, 2906.

2. (a) V. Elayappan, P. A. Shinde, G. K. Veerasubramani, S. C. Jun, H. S. Noh, K. Kim, M. Kim, H. Lee, *Dalton Trans.*, 2020, Advance Article, DOI:10.1039/C9DT04522H; (b) T. Mehtab, G. Yasin, M. Arif, M. Shakeel, R. M. Korai, M. Nadeem, N. Muhammad, X. Lu, *J. Energy Storage*, 2019, **21**, 632; (c) X. Zhang, A. Chen, M. Zhong, Z. Zhang, X. Zhang, Z. Zhou, X.-H. Bu, *Electrochem. Energ. Rev.*, 2019, **2,** 29.

3. (a) Y. Ye, J. Du, L. Sun, Y. Liu, S. Wang, X. Song, Z. Liang, *Dalton Trans*., 2020, Advance Article, DOI:10.1039/C9DT04305E; (b) P. Pullumbi, F. Brandani, S. Brandani, *Curr. Opin. Chem. Eng.* 2019, **24,** 131; (c) P. Gómez-Álvarez, S. Hamad, M. Haranczyk, A. R. Ruiz-Salvador, S. Calero, *Dalton Trans*., 2016, **45**, 216; (d) T. A. Makal, J. R. Li, W. Lu, H. C. Zhou, *Chem. Soc. Rev.*, 2012, **41**, 7761; (e) M. P. Suh, H. J. Park, T. K. Prasad, D. W. Lim, *Chem. Rev*., 2012, **112**, 782; (f) P. Cui, Y.G. Ma, H. H. Li, B. Zhao, J. R. Li, P. Cheng, P. B. Balbuena, H. C. Zhou, *J. Am. Chem. Soc*., 2012, **134**, 18892.

4. (a) P. Verma, U. P. Singh, R. J. Butcher, *CrystEngComm*, 2019, **21**, 5470; (b) L. X. You, Y. Guo, S.Y. Xie, S. J. Wang, G. Xiong, I. Dragutan, V. Dragutan, F. Ding, Y.G. Sun, *J. Solid State Chem*., 2019, **278.** https://doi.org/10.1016/j.jssc.2019.120900; (c) P. Verma, U. P. Singh, R. J. Butcher, *CrystEngComm*, 2019, **21**, 5470 (d) L. X. You, B. B. Zhao, H. J. Liu, S.J. Wang, G. Xiong, Y. K. He, F. Ding, J. J. Joos, P. F. Smet, Y. G. Sun, *CrystEngComm*, 2018, **20**, 615; (e) Y.N. Sun, G. Xiong, V. Dragutan, I. Dragutan, F. Ding, Y.G. Sun, *Inorg. Chem. Commun*. 2015**, 62**, 103; (f) J. Rocha, L. D. Carlos, F. A. A. Paz, D. Ananias, *Chem. Soc. Rev*., 2011, **40**,926; (g) Y. J. Cui, Y. F. Yue, G. D. Qian, B. L. Chen, *Chem. Rev*., 2012, **112**, 1126; (h) S. K. Mandal, H. W. Roesky, *Acc. Chem. Res*., 2010, **43**,248.

5 (a) X. J. Feng, W. Z. Zhou, Y. G. Li, H. S. Ke, J. K. Tang, R. Clerac, Y. H. Wang, Z. M. Su, E. B. Wang, *Inorg. Chem*., 2012, **51**, 2722; (b) L. Sorace, C. Benelli, D. Gatteschi, *Chem. Soc. Rev*.2011, **40**,

3092; (c) K. Biradha, C. Y. Su, J. J. Vittal, *Cryst. Growth Des*., 2011, **11**,875.

6. (a) Z. Liu, L. Ning, K. Wang, L. Feng, W. Gu, X. Liu, *Dalton Trans*.**,** 2020, Advance Article, doi: 10.1039/C9DT04051J; (b) A. Bavykina, N. Kolobov, I. S. Khan, J. A. Bau, A. Ramirez, J. Gascon, *Chem. Rev.* 2020, Article ASAP, doi:10.1021/acs.chemrev.9b00685; (c) A. L. Semrau, Ph. M. Stanley, A. Urstoeger, M. Schuster, M. Cokoja, R. A. Fischer, *ACS Catalysis,* 2020**, 10**, 3203; (d) V.Pascanu, G. González Miera, A. Ken Inge, B. Martín-Matute, *J. Am. Chem. Soc.*, 2019, **141**, 7223; (e) D. Yang, B.C. Gates*, ACS Catal.* 2019, **9**, 1779; (f) S. Luo, Z. Zeng, G. Zeng, Z. Liu, R. Xiao, M. Chen, L. Tang, W. Tang, C. Lai, M. Cheng, B. Shao, Q. Liang, H. Wang, D. Jiang, *ACS Appl. Mater. Interfaces* 2019*,* **11**, 32579; (g) Zh. Chen, K. Ma, J. J. Mahle, H. Wang, Z. H. Syed, A. Atilgan, Y. Chen, J. H. Xin, T. Islamoglu, G. W. Peterson, O. K. Farha, *J. Am. Chem. Soc.,* 2019, **141**, 20016.

7 (a) A.V. Desai, S. Sharma, S. Let, S.K. Ghosh, *Coord. Chem. Rev*., 2019, **395**, 146; (b) R.-B. Lin, Sh. Xiang, B. Li, Y. Cui, G. Qian, W. Zhou, B. Chen, *Coord. Chem. Rev*., 2019, **384**, 21; (c) A. H. Chughtai, N. Ahmad, H. A. Younus, A. Laypkov, F. Verpoort, *Chem. Soc. Rev*., 2015, **44**, 6804; (d) Y.S. Kang, Y. Lu, K. Chen, Y. Zhao, P. Wang, W.Y. Sun, *Coord. Chem. Rev*., 2019, **378**, 262.; (e) A. Dhakshinamoorthy, H. Garcia, *Chem. Soc. Rev*., 2014, **43**, 5750.

8 (a) Q. Wang, D. Astruc, *Chem. Rev.*, 2020**, 120**, 1438; (b) S. C. Shit, R. Singuru, S. Pollastri, B. Joseph, B. S. Rao, N. Lingaiah, J. Mondal, *Catal. Sci. Technol*., 2018, **8**, 2195; (c) P. Sudarsanam, R. Y. Zhong, S. V. den Bosch, S. M. Coman, V. I. Parvulescu, B. F. Sels, *Chem. Soc. Rev*., 2018, **47**, 8349; (d) X. M. Liu, B. Tang, J. L. Long, W. Zhang, X. H. Liu, Z. Mirza, *Sci. Bul.*, 2018, **63**, 502; (e) G. Xiong, X. L. Chen, L. X. You, B. Y. Ren, F. Ding, I. Dragutan, V. Dragutan, Y. G. Sun, *J. Catal*., 2018, **361**, 116; (f) F. M. Zhang, S. Zheng, Q. Xiao, Y. J. Zhong, W. D. Zhu,A. Lin, M. S. El-Shall, *Green Chem*., 2016, **18**, 2900; (g) Z. Liu, L. Ning, K. Wang, L. Feng, W. Gu, X. Liu, *Dalton Trans*., 2020, Advance Article, DOI: 10.1039/C9DT04051J; (h) X. Sun, K. Yuan, Y. Zhang, *J. Rare Earths*, 2020, https://doi.org/10.1016/j.jre.2020.01.012.

9 (a) L. X. You, L. X. Cui, B. B. Zhao, G. Xiong, F. Ding, B. Y. Ren, Z. L. Shi, I. Dragutan, V. Dragutan, Y. G. Sun, *Dalton Trans*., 2018, **47**, 8755; (b) L. X. You, H. J. Liu, L. X. Cui, F. Ding, G. Xiong, S. J. Wang, B. Y. Ren, I. Dragutan, V. Dragutan, Y. G. Sun, *Dalton Trans.* 2016, **45**, 18455; (c) L. X. You, W. H. Zong, G. Xiong, F. Ding, S. J. Wang, B. Y. Ren, I. Dragutan, V. Dragutan, Y. G. Sun, *Appl. Catal. A: Gen.,* 2016, **511**, 1; (d) L. X. You, W. L. Zhu, S. J. Wang, G. Xiong, F. Ding, B. Y. Ren, I. Dragutan, V. Dragutan, Y. G Sun, *Polyhedron,* 2016, **115**, 47; (e) S. L. Huang, A. Q. Jia, G. X. Jin, *Chem. Commun.,* 2013, **49**, 2403; (f) L. Wang, W. Yang, F. Y. Yi, H. Wang, Z. Xie, J. Tang, Z. M. Sun, *Chem. Commun.,* 2013, **49**, 7911; (g) A. Biffis, P. Centomo, A. Dell Zotto, M. Zecca, *Chem. Rev*., 2018, **118**, 2249; (h) I. Beletskaya, F. Alonso, V. Tyurin, *Coord. Chem. Rev*., 2019**, 385**, 137; (i) L. Liu, A. Corma, *Chem. Rev.,* 2018, **118**, 10, 4981; (j) J. El-Maiss, T. M. El Dine, C. S. Lu, I. Karamé, A. Kanj, K. Polychronopoulou, J. Shaya, *Catalysts,* 2020, **10**, 296.

10 (a) X. B. Lu, D. J. Darensbourg, *Chem. Soc. Rev*., 2012, **41**, 1462; (b) M. He, Y. Sun, B. Han, *Angew. Chem. Int. Ed*., 2013, **52**, 9620; (c) C. Martin, G. Fiorani, A. W. Kleij, *ACS Catal*., 2015, **5**, 135; (d) K. Sołtys-Brzostek, M. Terlecki, K. Sokołowski, J. Lewiński, *Coord. Chem. Rev*., 2017, **334**, 199; (e) A. J. Kamphuis, F. Picchioni, P. P. Pescarmona*, Green Chem.*, 2019, **21**, 406; (f) C. C. Yan, L. Lin, G. X. Wang, X. H. Bao, *Chin. J. Catal*., 2019, **40**, 23; (g) J. Septavaux, C. Tosi, P. Jame, C. Nervi, R. Gobetto, J. Leclaire, *Nat. Chem*., 2020, **12**, 202.

View Article Online
DOI: 10.1039/D0DT00770F

11 (a) M. Aresta, A. Dibenedetto, A. Angelini, *Chem. Rev.,* 2014, **114**, 1709; (b) Y. Tsuji, T. Fujihara, *Chem. Commun*., 2012, **48**, 9956; (c) N. Kielland, C. J. Whiteoak, A. W. Kleij, *Adv. Synth. Catal*., 2013, **355**, 2115; (d) N. Oncel, V. T. Kasumov, E. Sahin, M. Ulusoy, *J. Organomet. Chem.*, 2016, **81**, 8; (e) X. Fu, D. Zhou, K. Wang, H. Jing, *J. CO_2 Util.*,2016, **14**, 31.

12 (a) D. B. Wang, Q. H. Tan, J. J. Liu, Z. L. Liu, *Dalton Trans*., 2016, **45**,18450; (b) F. Guo, Y. P. Wei, S. Q. Wang, X. Y. Zhang, F. M. Wang, W. Y. Sun, *J. Mater. Chem. A***,** 2019, **7**, 26490.

13.(a) D. Astruc, "Organometallic Chemistry and Catalysis", Springer, 2007, Ch. 21, pp. 505-507; (b) F. Ding, Y. Li, P. Yan, Y. Deng, D. Wang, Y. Zhang, I. Dragutan, V. Dragutan, K. Wang, *Molecules*, 2018***, 23,*** 2435; (c) T. Ichikawa, M. Netsu, M. Mizuno, T. Mizusaki, Y. Takagi, Y. Sawama, Y. Monguchi, H. Sajiki, *Adv. Synth. Catal.*, 2017, **13**, 2269; (d) S. Calero, P. Gómez-Álvarez, *J. Phys. Chem. C*, **2015**, *119*, 23774; (e) C. F. R. A. C. Lima, A. S. M. C. Rodrigues, V. L. M. Silva, A. M. S. Silva, M. N. B. F. Santos, *ChemCatChem.*, 2014, **6**, 1291; (f) Ch. Amatore, G. Le. Duc, A. Jutand, *Chem Eur. J.*, 2013, **19**, 10082.

14. (a) Y. Shi, S. Hou, X. Qiu, B. Zhao, *Top Curr Chem (Z),* 2020, **378**, DOI:10.1007/s41061-019-0269-9; (b) Sh.-L. Hou, J. Dong, B. Zhao, *Adv. Mater.*, 2019, 1806163, DOI: 10.1002/adma.201806163 and ref. therein; (c) Q. Liu, L. Wu, R. Jackstell, M. Beller, "Using carbon dioxide as a building block in organic synthesis", *Nat. Commun*., 2015, **6**, 1 and ref. therein.

15. M. D. Burkart, N. Hazari, C. L. Tway, E. L. Zeitler, *ACS Catal.*, 2019, **9**, 7937. DOI: 10.1021/acscatal.9b02113.

16. M. Ding, H. L. Jiang, *ACS Catal.*, 2018, **8**, 3194. DOI: 10.1021/acscatal.7b03404.

17. (a) B. M. Trost, S. R. Angle, *J. Am. Chem. Soc.* 1985, **107**, 21, 6123; (b) X. Fu, D. Zhou, K. Wang, H. Jing, *J.* CO_2 *Util*., 2016, **14** 31. DOI: 10.1016/j.jcou.2016.02.003; (c) J. B. dela Cruz, M. Ruamps, S. Arco, C.-H. Hung, *Dalton Trans.*, 2019, **48**, 7527.18.

18. R. Khatun, P. Bhanja, P. Mondal, A. Bhaumik, D. Das, Sk. M. Islam, *New J. Chem.*, 2017, **41**, 12937.

19. S. Senthilkumar, M. S. Maru, R. S. Somani, H. C. Bajaj, S. Neogi, *Dalton Trans.*, 2018, **47,** 418.

20. (a) W. Y. Gao, Y. Chen, Y. H. Niu, K. Williams, L. Cash, P. J. Perez, L. Wojtas, J. F. Cai, Y. S. Chen, S. Q. Ma, *Angew. Chem. Int. Ed.*, 2014, **53**, 2615; (b) J. Liang, Y. B. Huang, R. Cao, *Coord. Chem. Rev.*, 2019, **378**, 32.

21. (a) D. Zhao, X. H. Liu, J. H. Guo, H. J. Xu, Y. Zhao, Y. Lu, W. Y. Sun, *Inorg. Chem*., 2018, **57**, 2695; (b) D. Zhao, X. H. Liu, C. Zhu, Y. Sh. Kang, P. Wang, Z. Shi, Y. Lu, W. Y. Sun, *ChemCatChem,* 2017, **9** 4598; (c) D. Zhao, X. H. Liu, Z. Z. Shi, C. D. Zhu, Y. Zhao, P. Wang, W. Y. Sun, *Dalton Trans.*, 2016, **45**, 14184.

22 J. Septavaux, C. Tosi, P. Jame, C. Nervi, R. Gobetto, J. Leclaire, *Nat. Chem.*, 2020, **12**, 202.

View Article Online
DOI: 10.1039/D0DT00770F

Graphical Abstract

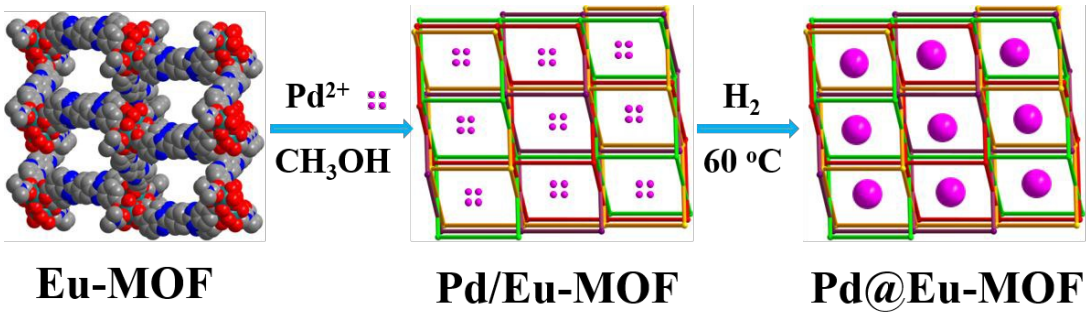

Pd@Eu-MOF nanocatalyst was obtained via solution impregnation and H_2 reduction and used in recyclable Suzuki-Miyaura reactions and chemical fixation of CO_2 to epoxides.